PERFORMANCE OF R-22 AND ITS ALTERNATIVES WORKING AT HIGH OUTDOOR TEMPERATURES

by

Samuel F. Yana Motta, Piotr A. Domanski
Building and Fire Research Laboratory
National Institute of Standards and Technology
Gaithersburg, MD 20899 USA

N I S T   C E N T E N N I A L ■

NIST
National Institute of Standards and Technology
Technology Administration, U.S. Department of Commerce

PERFORMANCE OF R-22 AND ITS ALTERNATIVES WORKING AT HIGH OUTDOOR TEMPERATURES

Samuel F. Yana Motta[1] and Piotr A. Domanski[2]

[1] Guest Researcher, E-mail: sssamuel@nist.gov, [2] E-mail: piotr.domanski@nist.gov
National Institute of Standards and Technology
100 Bureau Drive, STOP 8631, Gaithersburg, MD 20899-8631, USA

ABSTRACT

This paper examines the performance of R-22 and its possible replacements in an air-cooled air conditioner. The study focuses on the effect of elevated outdoor temperatures on system capacity and coefficient of performance (COP). The refrigerants considered are R-22, R-134a, R-290, R-410A and R-407C. Relative merits of these fluids are evaluated using the UA version of NIST's semi-theoretical vapor-compression model CYCLE-11. The study includes performance results for the basic cycle and for the cycle with a liquid-line/suction-line heat exchanger. The examined refrigerants exhibit varying degradations in performance at elevated temperatures compared to their performance at a typical operating regime. Different refrigerants' critical temperatures and differences in the shape of the two-phase dome on the temperature-entropy diagram can explain different performance trends for the refrigerants studied.

INTRODUCTION

This paper presents simulation results on performance of R-22 and four possible replacements (R-134a, R-290, R-410A and R-407C) at high outdoor temperatures. Previous studies reported an increased degradation of performance for fluids having a low critical temperature (e.g., R-410A), so an attempt to explain this behavior is included. In addition, this study explores a possible way to mitigate such degradation in performance by using a suction-line/liquid-line heat exchanger (llsl-hx).

A refrigerant's critical temperature (along with the molar heat capacity) is one of the two fundamental thermodynamic properties affecting refrigerant performance in the vapor compression cycle (e.g., McLinden, 1987, Domanski, 1999). For a given application, a fluid with a lower critical temperature will tend to have a higher volumetric capacity and a lower coefficient of performance (COP). The difference in COPs is related to different levels of irreversibility on the superheated-horn side and at the throttling process, as shown conceptually in Figure 1. These levels of irreversibility vary with operating temperatures because the slopes of the saturated liquid and vapor lines change, particularly when approaching the critical point.
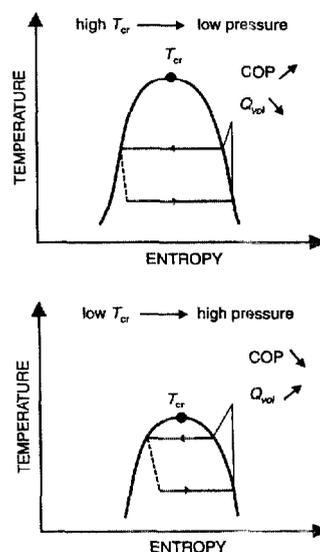

Figure 1. Impact of critical temperature on volumetric capacity and COP.

Meurer et al. (1999) compared the performances of R-22 and R-410A, working at elevated condensing temperatures up to 60 °C. The components of the system were an open reciprocating compressor, a water-cooled condenser, a methanol-heated evaporator, a thermostatic expansion valve, and a liquid-line accumulator. The authors reported the R-410A compressor having higher isentropic (+14 %) and volumetric (+22 %) efficiencies than R-22. COP of R-410A was higher by 16 % than R-22 COP at a typical operating condition (27 °C condensing temperature and 9 °C evaporation temperature), but it was lower by 1 % at a higher condensing temperature operating condition (57 °C condensing temperature and 9 °C evaporation temperature). The authors stated that a lower compressor speed accounted for part of the benefits measured with R-410A. Hence, the use of equal rotational speed would negatively affect the R-410A compressor and system performance.

Chin and Spatz (1999) explored some of the advantages and disadvantages of R-410A application in air conditioning systems. They used compressor performance data and a heat pump simulation model to compare R-22 and R-410A. In this study, they also performed heat exchangers' optimization to exploit the favorable thermophysical properties of R-410A. The authors concluded that the superior performance of the R-410A compressor and optimized heat exchangers compensated for the lower thermodynamic efficiency of R-410A relative to R-22 at low and moderate condensing temperatures. However, the R-410A system experienced a loss in COP relative to the R-22 system at condensing temperatures exceeding 47 °C.

SIMULATION MODEL

CYCLE-11 is a semi-theoretical model for evaluating the performance of refrigerants or refrigerant mixtures in the vapor-compression cycle (Domanski and McLinden, 1992, Domanski et al., 1994b). The model performs simulations for user-specified temperature profiles of the heat source and heat sink. The simulated system includes the compressor, evaporator, condenser, isenthalpic expansion device, and a liquid-line/suction-line heat exchanger. The user may specify a cross-flow, counter-flow, and parallel-flow evaporator and condenser with refrigerant superheat and subcooling, where appropriate. The program employs FORTRAN subroutines from REFPROP 6.01 (McLinden et al., 1998) to calculate refrigerant thermophysical properties.

In the UA version of CYCLE-11 used in this study, the evaporator and condenser are represented by their UA values, a product of the overall heat-transfer coefficient (U) and heat-transfer area (A). The model can account for different refrigerant-side heat-transfer coefficient and pressure drop in the evaporator and condenser, as they occur due to different refrigerant mass fluxes and properties at different operating conditions for the same refrigerant, or due to different thermophysical properties for different fluids. These differences are evaluated on a relative basis using a reference-case operating condition for which evaporator and condenser UA values are specified (Domanski et al., 1994).

CYCLE-11 employs inside-tube flow correlations for heat transfer and pressure drop calculations. For the evaporation heat-transfer coefficient, the model uses the complete form (the boiling and convective terms) of the Thome et al. (1996) correlation, because it was validated with diverse fluids, including zeotropic mixtures. For the condensation heat-transfer coefficient, we selected the relative old correlation of Shah (1979), because it shows good agreement with experimental data for various fluids, as reported by Eckels et al. (1998). The Shah correlation is also convenient to use because it reduces to the Dittus-Boelter correlation for the single-phase flow.

The model predicts pressure drop using the new NIST correlation (Choi et al., 1999). This correlation was validated for evaporation and condensation with pure refrigerants and mixtures using

three independent sources of experimental data. CYCLE-11 uses only the frictional term, which has been rearranged to become a function of an empirical parameter, geometry, and fluid properties. The value of the empirical constant is calculated at the outset using the imposed pressure drop at the reference-case operating condition.

The liquid-line/suction-line heat exchanger (llsl-hx) is assumed to be a counter-flow heat exchanger. The model predicts pressure drop and heat transfer by applying the scheme used for the evaporator and condenser, i.e., by obtaining empirical pressure drop and heat transfer parameters based on the reference-case performance, and extrapolating the performance using single-phase pressure drop and Dittus-Boelter heat transfer correlations.

Table 1. Selected properties of studied refrigerants

Parameter	R-22	R-134a	R-290	R-410A	R-407C
Critical Temperature [°C]	96.1	101.0	96.7	70.2	86.1
Temperature Glide*	0	0	0	0.1	6.0
Evaporation Pressure* [kPa]	640.9	387.6	601.1	1021.0	666.0
Volumetric Capacity* [kJ/m³]	5386.6	3644.1	4732.2	8296.2	5865.6
Liquid Molar Heat Capacity* [kJ/kmol·K]	103.2	139.2	113.5	112.7	123.1
Liquid Thermal* Conductivity [W/m·K]	0.0913	0.0885	0.1014	0.1090	0.0982
Liquid Dynamic* Viscosity [μPa·s]	200.0	244.9	116.2	150.4	196.4
Liquid Surface Tension* [N/m]	0.0105	0.0104	0.0091	0.0075	0.0099

* Properties evaluated at 8 °C average evaporation temperature

REFRIGERANTS STUDIED

Table 1 shows selected properties of the refrigerants studied. R-410A has a significantly lower critical temperature than R-22 and other fluids. For this reason, R-410A will have the highest pressure in the system, as is shown by the evaporation pressure in table 1. Because it has the highest evaporator pressure, R-410A has the highest volumetric capacity. Regarding transport properties, R-410A has a superior balance of liquid conductivity, viscosity, and surface tension, which justifies the high values of heat transfer coefficients for R-410A reported by previous studies (e.g. Bivens et al., 1993).

Figures 2, 3, are temperature-entropy diagrams, and Figure 4 is a temperature-enthalpy diagram for the refrigerants studied. Figure 2 uses the molar entropy scale of kJ/kmol·K. In this figure, the slopes of saturation lines correlate with molar heat capacities, i.e., R-134a having the highest molar heat capacity has the smallest slope (see Table 1 for liquid molar heat capacities).
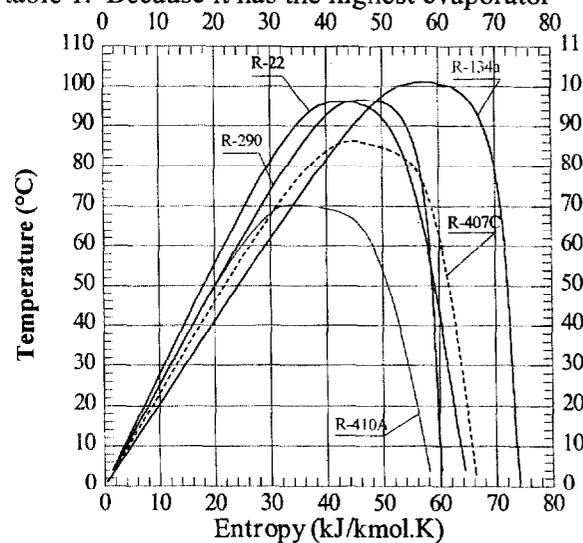

Figure 2. Temperature-entropy diagram.

Figures 3 and 4 use dimensionless entropy (s^*) and enthalpy (h^*) scales, respectively, for the horizontal axes. These dimensionless scales are referenced to the property change between saturated vapor and liquid at 0 °C, as given by the following two relations:

$$s^* = \frac{s - s_l^0}{s_v^0 - s_l^0} \qquad h^* = \frac{h - h_l^0}{h_v^0 - h_l^0} \qquad (1)$$

where:

s, h = entropy and enthalpy,

s_v^0, h_v^0 = entropy and enthalpy of saturated vapor at 0 °C,

s_l^0, h_l^0 = entropy and enthalpy of saturated liquid at 0 °C.

Figures 3 and 4 are suitable for qualitative analysis of the impact of the shape of the two-phase dome on the coefficient of performance because the width of the two-phase dome is normalized. If we envisage vapor-compression cycles and corresponding Carnot cycles drawn for each refrigerant with the same condensing and evaporating temperatures, we can conclude that the superheated-vapor-horn irreversibilities (Figure 3) and throttling-induced capacity losses (Figure 4) will be greater for R-410A than for R-22 due to R-410A's smaller dome.
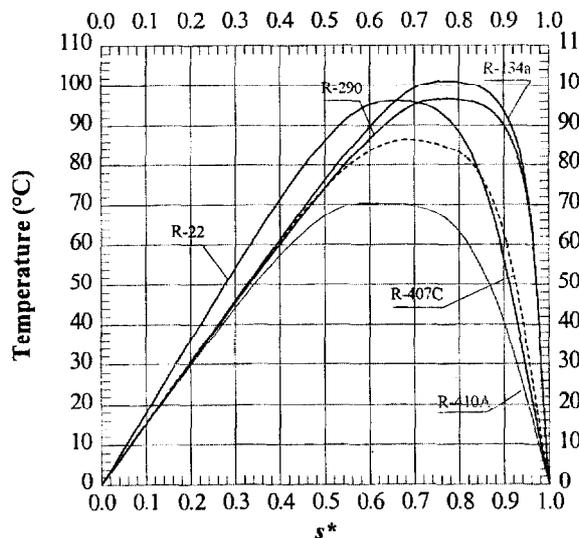

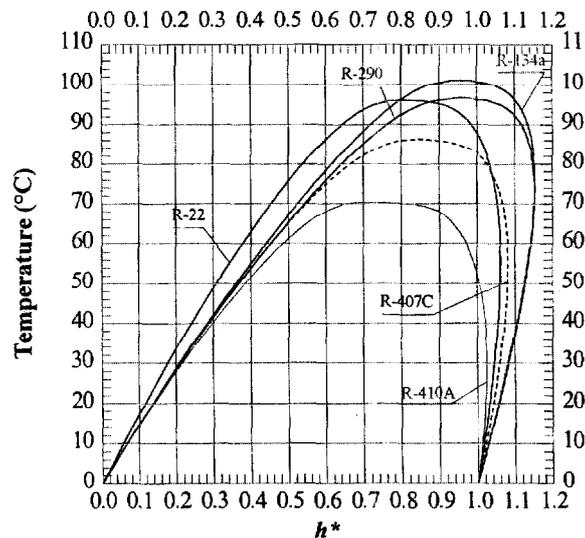Figure 3. Temperature-dimensionless entropy diagram.

Figure 4. Temperature-dimensionless enthalpy diagram.

COMPARISON BASES

Simulated System

All the fluids employed reciprocating-type compressors. The common characteristics of these compressors were: rotational speed of 1800 rpm, electric motor efficiency of 0.9, and polytropic efficiency of 0.7. The volumetric efficiency was simulated with a common relation used for reciprocating compressors (Domanski and McLinden, 1992). The compressors had different cylinder swept volumes, so each studied refrigerant matched the cooling capacity of the R-22 system (12.66 kW) at the reference-case operating condition (see values in Table 2).

For all five studied refrigerants, we used physically the same condenser and evaporator, which were of a cross-flow configuration. We started our simulations with R-22 at the reference-point operating condition, which we defined by the following air temperatures: 26.7 °C at evaporator inlet, 14.4 °C at evaporator outlet, 35.0 °C at condenser inlet, and 43.3 °C at condenser outlet. For this simulation point, we imposed the *UA* values for the evaporator and condenser to obtain realistic temperature differences between air and R-22. We also imposed the refrigerant circuitry to obtain a realistic pressure drop. For other operating conditions and fluids, refrigerant heat transfer and pressure drop were simulated, while the heat transfer resistance on the air-side and air volumetric flow rates remained unchanged. In these non-reference-point simulations, the air temperature at the evaporator inlet was always 26.7 °C, while we used different condenser inlet-air temperatures from 25.0 °C to 55.0 °C. The air outlet temperatures in the condenser and evaporator were calculated from the energy balance between refrigerant and air. For all simulations, the evaporator superheat and condenser subcooling were held at 5 °C. Table 2 includes refrigerant-side heat transfer coefficients, *UA* values, and pressure drops simulated for the operating condition with 35 °C outdoor temperature.

Table 2. System parameters at 35 °C air temperature at the condenser inlet

Refrigerants	R-22	R-134a	R-290	R-410A	R-407C
Compressor Displacement* [m³·10⁶]	114.0	181.8	134.5	77.4	113.9
UA, Condenser** [kW/K]	2.100	2.147	2.174	2.213	2.139
UA, Evaporator** [kW/K]	1.140	1.161	1.164	1.166	1.153
Refrig. Heat-Transfer Coeff., Evaporator [kW/m²·K]	5.135	5.849	5.966	6.045	5.558
Refrig. Heat-Transfer Coeff., Condenser [kW/m²·K]	3.080	3.349	3.520	3.790	3.301
Refrig. Mass Flux, Evaporator & Condenser [kg/m²·s]	299.5	322.0	171.4	295.6	300.7
Condenser Pressure Drop** [kPa]	15.0	22.2	12	9.4	13.4
Evaporator Pressure Drop** [kPa]	15.0	25.5	11.6	10.3	15.4
Condensing Temperature (calculated) [°C]	46.3	46.7	46.7	45.7	46.7
Evaporation Temperature (calculated) [°C]	8.2	8.4	8.4	8.4	8.15
COP	3.65	3.65	3.69	3.55	3.57
Additional Parameters for llsl-hx					
llsl-hx Effectiveness**	0.6	0.563	0.529	0.525	0.551
Pressure Drop, Liquid Side of llsl-hx** [kPa]	1.0	1.164	0.804	1.008	1.058
Pressure Drop, Vapor Side of llsl-hx** [kPa]	3.0	4.858	2.131	2.039	3.02
UA, llsl-hx [kW/K]	0.064	0.075	0.072	0.073	0.0723
COP	3.677	3.701	3.748	3.586	3.603

* Imposed for R-22. Calculated for other fluids to obtain R-22 cooling capacity (12.66 kW).
** Imposed for the reference case with R-22. Simulated for other operating conditions and fluids.

For simulations with the llsl-hx, we used physically the same heat exchanger. We imposed the effectiveness of 60 % for the R-22 reference-case operating condition. The geometry of the llsl-hx was such that the vapor-side pressure drop was 3.0 kPa, and the liquid-side pressure drop was 1.0 kPa. For other refrigerants and operating conditions, the effectiveness and pressure drops were simulated. The values of system parameters shown in Table 2 reflect the impact of properties on heat transfer, pressure drop, and COP at the 35 °C air outdoor temperature.

SIMULATION RESULTS

Basic Cycle (no llsl-hx)

Figure 5 shows simulation results for R-22 and R-410A systems. The COP of R-410A is lower than that of R-22, and the difference is getting larger at higher outdoor temperatures. This is a result of the larger decrease of R-410A capacity as the trends of compressor power for both fluids are the similar. The stronger degradation in capacity for R-410A (a low-critical-temperature fluid) can be deduced from Figure 4. It becomes evident, that the throttling process cuts more significantly into the two-phase dome (and reduces the refrigerating effect), when the condensing temperature approaches the critical point, as it is the case for R-410A. Regarding the compressor, the impact of increased condensing pressure is not much different for all fluids. This is because the compressor is not affected by the proximity of the critical point and a change in shape of the thermodynamic cycle, but responds only to a change in the discharge pressure (refrigerant suction density and pressure were not changed significantly).
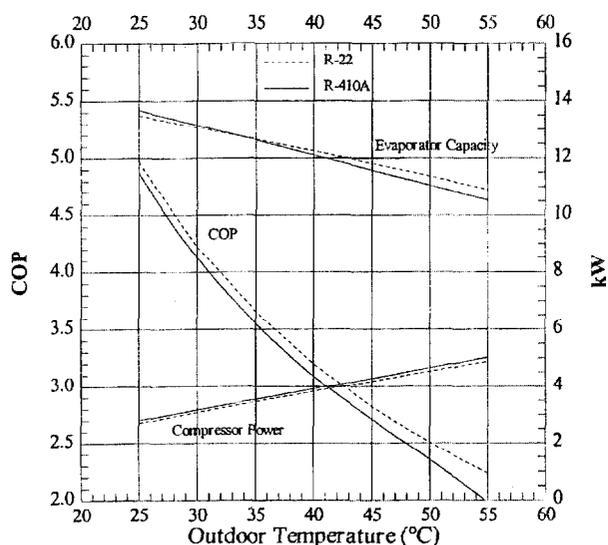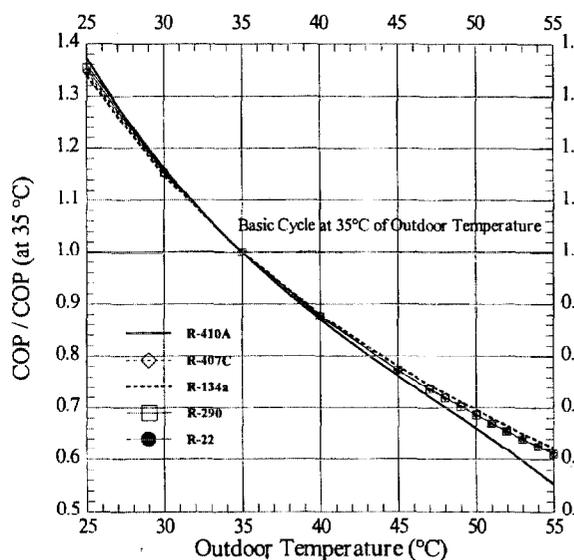
Figure 5. Performance of R-22 and R-410A systems.

Figure 6. COP referenced to COP at 35 °C.

Figure 6 shows changes of COP for each refrigerant for different outdoor temperatures. The COP values are normalized by the COP at 35 °C for each fluid. R-410A has the highest degradation in COP and R-134a has the lowest one. The lines representing the performance of R-410A (the lowest-critical-temperature fluid) and R-134a (the highest-critical-temperature fluid) bracket the performance of the remaining refrigerants. The change of COP for R-22, R-290, and R-407C is very similar, because their critical temperatures are within 10 °C of each other.

Figure 7 presents the COP of the four alternatives normalized by the COP of the R-22 system. R-134a, the fluid with the highest critical temperature, improves its performance in relation to R22. On the other hand, the COP of R-410A drops dramatically at increasing outdoor temperature. Regarding the fluids with similar critical temperatures to R-22 (R-407C and R-290), the small COP differences are caused by the different shape of the two-phase domes of these fluids rather than their different critical temperatures.
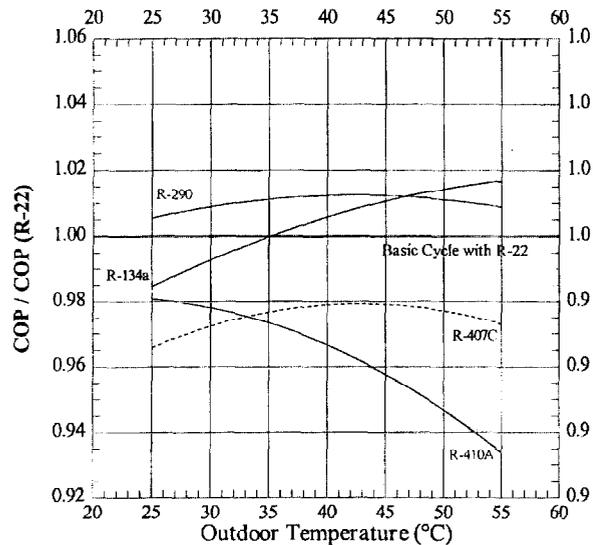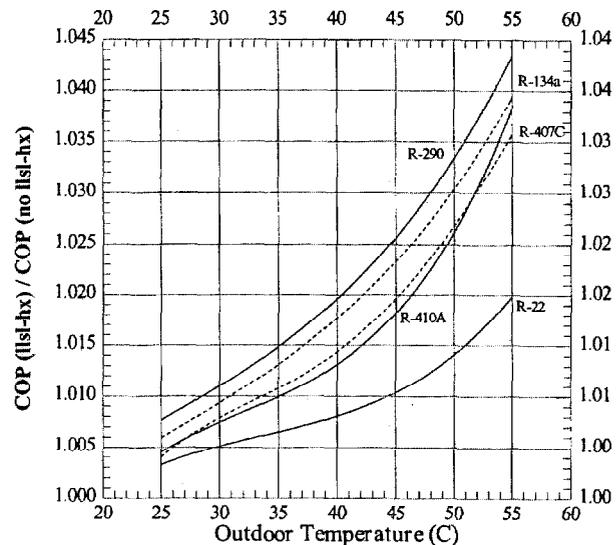
Figure 7. COP referenced to COP of R-22 system. Figure 8. COP for llsl-hx cycle referenced to COP for basic cycle.

Cycle with llsl-hx

The benefit of using the llsl-hx depends on the refrigerant's molar heat capacity, which affects the slope of the saturation lines on the temperature-entropy diagram (Domanski et al. 1994a). Fluids with a large molar heat capacity tend to have larger throttling losses, which can be somewhat minimized by the use of a llsl-hx. Since the slope of the saturation liquid line changes significantly when the critical temperature is approached, we examined the potential benefit of the llsl-hx at higher outdoor air temperatures.

Figure 8 shows COPs in the llsl-hx cycle normalized by the COP of the basic cycle for each fluid. We used physically the same llsl-hx for each fluid, and accounted for some pressure drop, which was different for different refrigerants, as shown in Table 2 for the 35 °C operating condition. All fluids benefited from the use of the llsl-hx. The degree of COP improvement correlates well with the molar heat capacity. The lines for R-290, R-134a, and R-407C have a similar trend, while the R-410A line assumes a steeper slope at outdoor temperatures greater than 45 °C. This change of slope indicates an improved benefit that may be a result of approaching the critical temperature. (See the saturated line of R-410A curving toward the critical point in Figure 2). However, the overall impact of approaching the critical point at up to 55 °C outdoor temperature is small. In addition, it may be noted that the COP improvement is greater for higher ambient temperatures. This higher llsl-hx benefit is consistent with a high-temperature-lift operation where more throttling irreversibility is available for recovery.

CONCLUDING REMARKS

Performance of a vapor compression system decreases with increasing outdoor temperatures. R-410A has more pronounced performance degradation than R-22, R-407C, R-290, and R-134a because of its low critical temperature. Simulations showed that fluids with a low critical temperature experience a larger degradation of cooling capacity, while rate of compressor power increase is similar for all fluids.

The use of a llsl-hx provided COP improvement for all refrigerants. For outdoor air temperatures studied (up to 55 °C), the COP improvement well correlated with the molar heat capacity of the refrigerants.

It should be noted that the study shows performance trends of five different refrigerants working in the systems that employed the same heat exchangers and compressors of the same efficiency. No optimization was carried out to optimize performance of individual fluids. R-410A in particular would benefit from heat exchangers' optimization because of (1) its small change in saturation temperature for a given pressure drop and (2) a postulated improved compressor efficiency due to the low pressure ratio. With system optimization, the absolute values of capacity and COP for different refrigerants would change; however, the performance trends would not be affected because they are referenced to the performance of each refrigerant at the reference-point operating condition.

ACKNOWLEDGEMENTS

REFERENCES

Bivens, D.B., Yokozeki, A., Geller, V.Z., and Paulaitis, M.E., Transport properties and heat transfer of alternatives for R-502 and R-22, ASHRAE/NIST Refrigerants Conference, August 1993, pp.73-84.

Chin, L. and Spatz, M.W., issues relating to the adoption of R-410A in air conditioning systems, 20th International Congress of Refrigeration, IIR/IIF, Sydney, 1999.

Choi, J.Y., Kedzierski, M.A., and Domanski, P.A, A Generalized Pressure Drop Correlation for Evaporation and Condensation of Alternative Refrigerants in Smooth and Micro-Fin Tubes, NISTIR 6333, U.S. Department of Commerce, Washington, D.C., 1999.

Domanski, P.A. and McLinden, M.O., A simplified cycle simulation model for the performance rating of refrigerants and refrigerant mixtures, Int. Journal of Refrigeration, Vol. 15, No 2, pp. 81-88, 1992.

Domanski, P.A., Didion, D.A., and Doyle J.P., Evaluation of suction-line/liquid-line heat exchange in the refrigeration cycle, International Journal Refrigeration, Vol. 17, No. 7, pp. 487-492, 1994a.

Domanski, P.A., Didion, D.A., Mulroy, W.J., and Parise, J.A.R., A Simulation Model and Study of Hydrocarbon Refrigerants for Residential Heat Pump Systems, IIR Conference on New Applications of Natural Working Fluids in Refrigeration and Air Conditioning, Germany, pp. 339-354, 1994b.

Domanski, P.A., Evolution of Refrigerant Application, International Congress of Refrigeration, Milan, Italy, May 4, 1999.

Eckels, S.J., Tesene, B., and Wang, Q., In-tube Condensation of Refrigerants in Smooth and Enhanced Tubes, ASHRAE New Investigator Project, 1998.

McLinden, M., Thermodynamic evaluation of Refrigerants in the Vapor Compression Cycle Using Reduced Properties, International Journal Refrigeration, Vol. 11, pp. 134-143, 1987.

McLinden, M.O., Klein, S.A., Lemmon, E.W., and Peskin, A.P., NIST Thermodynamic and Transport Properties of Refrigerants and refrigerant Mixtures – REFPROP (Version 6.01), National Institute of Standards and Technology – Physical and Chemical Properties Division (Boulder, Colorado), 1998.

Meurer, C., Buyle, O., and Paulus-Lanckriet, M., Comparison of R-22 and R-410A at elevated condensing temperatures, 20th International Congress of Refrigeration, IIR/IIF, Sydney, 1999.

Shah, M., A generalized correlation for heat transfer during film condensation inside pipes, International Journal of Heat and Mass Transfer, Vol. 22, pp. 547-556, 1979.

Thome J.R., Heat transfer and pressure drop in the dryout region of intube evaporation with refrigerant/lubricant mixtures, ASHRAE Project 800-RP, 1996.